Transition properties of low-lying states in atomic indium

B. K. Sahoo*
Theoretical Physics Division, Physical Research Laboratory, Ahmedabad-380009, India

B. P. Das
Theoretical Astrophysics Group, Indian Institute of Astrophysics, Bangalore-560034, India

(Received 9 March 2011; published 6 July 2011)

We present here the results of our relativistic many-body calculations of various properties of the first six low-lying excited states of indium. The calculations were performed using the relativistic coupled-cluster method in the framework of the singles, doubles, and partial triples approximation. The lifetime of the $[4p^6]5s^2 5p_{3/2}$ state in this atom is determined. Our results could be used to shed light on the reliability of the lifetime measurements of the excited states of atomic indium that we have considered in the present work.

DOI: 10.1103/PhysRevA.84.012501 PACS number(s): 31.15.ag, 31.15.bw, 32.70.Cs

I. INTRODUCTION

Indium (In) was laser cooled and trapped a few years ago [1]. Following this experiment, a proposal was made to search for the permanent electric dipole moment (EDM) in this atom [2]. It would indeed be desirable to carry out high precision measurements and many-body calculations of other properties of this atom. A few measurements of the magnetic dipole hyperfine structure constants of the first three low-lying states of In are already available [3,4]. However, the reported theoretical results obtained using different variants of the relativistic coupled-cluster (RCC) method at the singles, doubles, and important triples excitations level [CCSD(T) method] are not able to reproduce them to within 1% accuracy [2,5]. This suggests that the role of correlation effects for this property is of crucial importance. In addition, it would also be worthwhile to calculate different transition amplitudes in In for a number of reasons. First of all, the behavior of the correlation effects in these properties could be quite different than in the hyperfine structure constants. Furthermore, these amplitudes in conjunction with the hyperfine constants can be employed to verify the accuracy of the wave functions for the proposed EDM calculations [2] or perhaps for parity nonconservation if at all an experiment to observe this effect is performed on this atom in the future and also to determine the polarizabilities, lifetimes, oscillator strengths, branching ratios, etc. for various states.

In this work, we calculate the excitation energies (EEs) and different transition amplitudes due to allowed and forbidden electromagnetic transitions among the first six low-lying states, giving a total of 34 possible transitions (see Fig. 1), using the relativistic CCSD(T) method. These results are further used to determine transition rates, branching ratios, and lifetimes of the above states. These properties are also important from an astrophysical point of view [6,7]. Safronova *et al.* have reported EEs and electric dipole ($E1$) transition amplitudes for a number of states and compared with previous calculations and measurements [5]. However, they have only considered these transition amplitudes to estimate the lifetimes of various states, but contributions from the forbidden transitions are not included. In our calculations, we have taken into account the forbidden transition amplitudes in the evaluation of the lifetimes of different states.

II. THEORY AND METHOD OF CALCULATIONS

The transition rates (in s^{-1}) due to various transitions are given by [8]

$$A^{E1}_{f\to i} = \frac{2.02613\times 10^{18}}{\lambda^3(2J_f+1)} S^{E1}_{f\to i}, \tag{2.1}$$

$$A^{M1}_{f\to i} = \frac{2.69735\times 10^{13}}{\lambda^3(2J_f+1)} S^{M1}_{f\to i}, \tag{2.2}$$

$$A^{E2}_{f\to i} = \frac{1.11995\times 10^{18}}{\lambda^5(2J_f+1)} S^{E2}_{f\to i}, \tag{2.3}$$

and

$$A^{M2}_{f\to i} = \frac{1.491\times 10^{13}}{\lambda^5(2J_f+1)} S^{M2}_{f\to i}, \tag{2.4}$$

where λ (in Å) and $S^{\rm O}_{f\to i}(=|\langle f||{\rm O}||i\rangle|^2)$ [in atomic unit (a.u.)] are the wavelengths and line strengths due to the corresponding transition operator O, respectively.

The lifetime (τ_f) of a given state f is just the reciprocal of the total transition rate of that state due to all possible transition channels, that is,

$$\tau_f = \frac{1}{\sum_{{\rm O},i} A^{\rm O}_{f\to i}}, \tag{2.5}$$

where $A^{\rm O}_{f\to i}$ is the transition rate due to operator O and sum over i and O represents the total transition rate from state f to all possible states i and due to all possible operators.

The branching ratios due to an operator O from a state f due to the lower states are given by

$$\Gamma^{\rm O}_{f\to i} = \frac{A^{\rm O}_{f\to i}}{\sum_{{\rm O},i} A^{\rm O}_{f\to i}} = \tau_f A^{\rm O}_{f\to i}. \tag{2.6}$$

*bijaya@prl.res.in

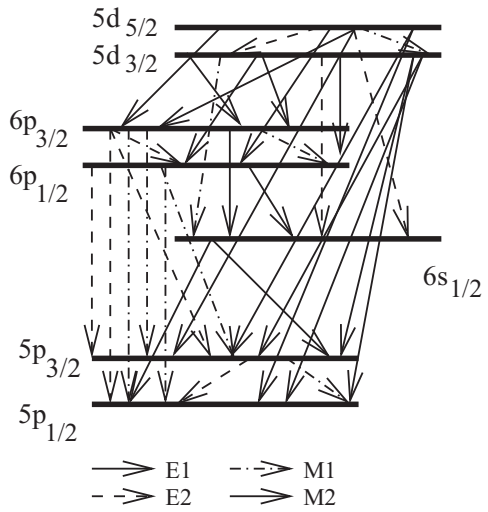

FIG. 1. Schematic low-lying energy level diagrams and decay channels of the low-lying states in In.

To evaluate the line strengths, we use the following reduced matrix elements at the single-particle orbitals level for the $E1$, $M1$, $E2$, and $M2$ operators [9]:

$$\langle \kappa_f \,||\, e1 \,||\, \kappa_i \rangle = \langle \kappa_f \,||\, C^{(1)} \,||\, \kappa_i \rangle \int_0^\infty drr \Big\{ (P_f P_i + Q_f Q_i) - \frac{\omega r}{5\alpha} \Big[\frac{\kappa_f - \kappa_i}{2} (P_f Q_i + Q_f P_i) + (P_f Q_i - Q_f P_i) \Big] \Big\}, \tag{2.7}$$

$$\langle \kappa_f || m1 || \kappa_i \rangle = \langle -\kappa_f \,||\, C^{(1)} \,||\, \kappa_i \rangle \int_0^\infty drr \frac{(\kappa_f + \kappa_i)}{\alpha} (P_f Q_i + Q_f P_i), \tag{2.8}$$

$$\langle \kappa_f \,||\, e2 \,||\, \kappa_i \rangle = \langle \kappa_f \,||\, C^{(2)} \,||\, \kappa_i \rangle \int_0^\infty drr^2 \Big\{ (P_f P_i + Q_f Q_i) - \frac{\omega r}{7\alpha} \Big[\frac{\kappa_f - \kappa_i}{3} (P_f Q_i + Q_f P_i) + (P_f Q_i - Q_f P_i) \Big] \Big\}, \tag{2.9}$$

and

$$\langle \kappa_f \,||\, m2 \,||\, \kappa_i \rangle = \langle -\kappa_f \,||\, C^{(2)} \,||\, \kappa_i \rangle \int_0^\infty drr^2 \frac{(\kappa_f + \kappa_i)}{3\alpha} (P_f Q_i + Q_f P_i), \tag{2.10}$$

where, j's and κ's are the orbital and relativistic angular momentum quantum numbers, respectively, P and Q represent the radial parts of large and small components of single-particle Dirac orbitals, respectively, $\omega = \epsilon_f - \epsilon_i$ for the orbital energies ϵs, α is the fine structure constant and the reduced Racah coefficients are given by

$$\langle \kappa_f \,||\, C^{(k)} \,||\, \kappa_i \rangle = (-1)^{j_f+1/2} \sqrt{(2j_f+1)(2j_i+1)}, \times \begin{pmatrix} j_f & k & j_i \\ 1/2 & 0 & -1/2 \end{pmatrix} \pi(l_{\kappa_f}, k, l_{\kappa_i}), \tag{2.11}$$

with

$$\pi(l,m,l') = \begin{cases} 1 & \text{for} \quad l+m+l' = \text{even} \\ 0 & \text{otherwise.} \end{cases} \tag{2.12}$$

In the above expressions and in the remaining part of the paper, we have used a.u. unless they are mentioned explicitly.

In order to determine the above properties, we calculate the atomic wave function ($|\Psi_v\rangle$) with a valence orbital v by expressing it in the RCC framework as

$$|\Psi_v\rangle = e^T \{1 + S_v\} |\Phi_v\rangle, \tag{2.13}$$

where we define a reference state $|\Phi_v\rangle$ by appending the appropriate valence orbital v to the Dirac-Fock (DF) wave function ($|\Phi_0\rangle$) with the configuration similar to cadmium, that is, $[4p^6]4d^{10}5s^2$. Here T and S_v represent the excitation operators due to core-core and core-valence electron correlations. In the CCSD(T) method, the T and S_v operators are defined as

$$T = T_1 + T_2 \quad \text{and} \quad S_v = S_{1v} + S_{2v}, \tag{2.14}$$

where 1 and 2 in the subscripts represent for single and double excitations, respectively.

The equations determining the coupled-cluster amplitudes and energy can be expressed in compact forms as

$$\langle \Phi_0^L | \{ \widehat{He^T} \} | \Phi_0 \rangle = \delta_{0,L} \Delta E_{\text{corr}}, \tag{2.15}$$

and

$$\langle \Phi_v^L | \{ \widehat{He^T} \} \{1 + S_v\} | \Phi_v \rangle = \langle \Phi_v^L | 1 + S_v | \Phi_v \rangle \langle \Phi_v | \{ \widehat{He^T} \} \{1 + S_v\} | \Phi_v \rangle = \langle \Phi_v^L | \delta_{L,v} + S_v | \Phi_v \rangle \Delta E_v, \tag{2.16}$$

where the superscript $L(=1,2)$ represents for the excited hole-particle states, $\widehat{He^T}$ denotes the connected terms of the Dirac-Coulomb (DC) Hamiltonian with the T operators, ΔE_{corr} and ΔE_v are the correlation energy and attachment energy [also equivalent to negative of the ionization potential (IP)] of the electron of orbital v, respectively. The reference states in Eqs. (2.15) and (2.16) contain a different number of particles, hence the Hamiltonian used in the respective equations describe a different number of particles in our Fock space representation. Contributions from the important valence triple excitations are included perturbatively through the above equations.

The transition matrix element of a physical operator O between $|\Psi_f\rangle$ and $|\Psi_i\rangle$ in our approach is given by

$$\frac{\langle \Psi_f | \mathrm{O} | \Psi_i \rangle}{\sqrt{\langle \Psi_f | \Psi_f \rangle} \sqrt{\langle \Psi_i | \Psi_i \rangle}} = \frac{\langle \Phi_f | \{1 + S_f^\dagger\} \overline{\mathrm{O}} \{1 + S_i\} | \Phi_i \rangle}{\sqrt{\langle \Phi_f | \overline{N} + S_f^\dagger \overline{N} S_f | \Phi_f \rangle} \sqrt{\langle \Phi_i | \overline{N} + S_i^\dagger \overline{N} S_i | \Phi_i \rangle}}, \tag{2.17}$$

where $\overline{\mathrm{O}} = e^{T^\dagger}\mathrm{O}e^{T}$ and $\overline{N} = e^{T^\dagger}e^{T}$ are two nontruncating series in the above expression. We evaluate them by considering terms whose leading contributions arise in fourth-order perturbation theory or lower. Contributions from the normalization of the wave functions ($\mathcal{N}$) are determined explicitly as follows:

$$\mathcal{N} = \frac{\langle\Psi_f|\mathrm{O}|\Psi_i\rangle}{\sqrt{\langle\Psi_f|\Psi_f\rangle}\sqrt{\langle\Psi_i|\Psi_i\rangle}} - \langle\Psi_f|\mathrm{O}|\Psi_i\rangle$$
$$= \langle\Psi_f|\mathrm{O}|\Psi_i\rangle\left[\frac{1}{\sqrt{\langle\Psi_f|\Psi_f\rangle}\sqrt{\langle\Psi_i|\Psi_i\rangle}} - 1\right]. \quad (2.18)$$

We have used Gaussian-type orbitals (GTOs) to construct the single-particle orbitals for the Dirac-Fock ($|\Phi_0\rangle$) wave function. The large and small components of the Dirac orbitals in this case are expressed as

$$P_\kappa(r) = \sum_k c_k^P r^{l_\kappa} e^{-\alpha_k r^2}, \quad (2.19)$$

and

$$Q_\kappa(r) = \sum_k c_k^Q r^{l_\kappa}\left(\frac{d}{dr} + \frac{\kappa}{r}\right) e^{-\alpha_k r^2}, \quad (2.20)$$

where the summation over k is for total number of GTOs used in each symmetry, c_k^P and c_k^Q are the normalization constants for the large and small components, respectively, and we use the $(\frac{d}{dr} + \frac{\kappa}{r})$ operator to expand the small component Dirac orbitals to maintain the kinetic balance condition with its large component. In the present calculations, we have considered nine relativistic symmetries (up to g symmetry) and 28 GTOs for each symmetry to generate the orbitals. In order to optimize the exponents to describe orbitals from various symmetries in a smooth manner, we use the even tempering condition:

$$\alpha_k = \alpha_0\beta^{k-1}, \quad (2.21)$$

where α_0 and β are two arbitrary parameters that can be chosen suitably for different symmetries. We have considered $\alpha_0 = 7.5 \times 10^{-4}$ for all the symmetries and β are taken as 2.53, 2.45, 2.58, 2.75, and 2.83 for s, p, d, f, and g orbitals, respectively. For the RCC calculations, we have considered excitations up to first $16s$, $16p$, $16d$, $14f$, and $13g$ orbitals as the remaining orbitals have large continuum energies.

TABLE I. IPs (ΔE_vs) of different states of In in cm^{-1}. Absolute error of our CCSD(T) results compared to the quoted results in [10] are given as Δ.

State	NIST[a] (cm^{-1})	Others[b] (cm^{-1})	Koopman[c] (cm^{-1})	CCSD(T)[c] (cm^{-1})	Δ (%)
$5p_{1/2}$	46670.11	46189	41521.74	46581.47	0.19
$5p_{3/2}$	44457.51	44031	39522.20	44361.04	0.22
$6s_{1/2}$	22297.15	22442	20567.70	22291.74	0.02
$6p_{1/2}$	14853.21	14833	13977.92	14819.07	0.23
$6p_{3/2}$	14554.89	14532	13718.04	14519.46	0.24
$5d_{3/2}$	13777.90	13581	12389.68	13633.48	1.05
$5d_{5/2}$	13754.57	13554	12373.64	13603.88	1.10

[a]Reference [10].
[b]Reference [5].
[c]This work.

TABLE II. Line strengths (in a.u.) due to allowed and forbidden transitions between different states in In. Numbers given in the parentheses and square brackets represent estimated errors and powers in 10, respectively.

Transition	DF	CCSD(T)	Others [5]
$5d_{5/2} \xrightarrow{E1} 6p_{3/2}$	251.95	188(2)	186
$5d_{5/2} \xrightarrow{M2} 6p_{3/2}$	4.9[3]	3.8(1)[3]	
$5d_{5/2} \xrightarrow{M2} 6p_{1/2}$	893.6	685(5)	
$5d_{5/2} \xrightarrow{E1} 5p_{3/2}$	20.55	16.3(5)	15.2
$5d_{5/2} \xrightarrow{M2} 5p_{3/2}$	399.59	474(10)	
$5d_{5/2} \xrightarrow{M2} 5p_{1/2}$	62.44	92(3)	
$5d_{5/2} \xrightarrow{M1} 5d_{3/2}$	2.40	2.41(1)	
$5d_{5/2} \xrightarrow{E2} 5d_{3/2}$	5.0[3]	2.9(2)[3]	
$5d_{5/2} \xrightarrow{E2} 6s_{1/2}$	9.4[3]	6.6(1)[3]	
$5d_{3/2} \xrightarrow{E1} 6p_{3/2}$	27.88	20(1)	20.5
$5d_{3/2} \xrightarrow{M2} 6p_{3/2}$	0.0	3.5(1)[−3]	
$5d_{3/2} \xrightarrow{E1} 6p_{1/2}$	139.07	104(5)	103
$5d_{3/2} \xrightarrow{M2} 6p_{1/2}$	83.44	65(3)	
$5d_{3/2} \xrightarrow{E1} 5p_{3/2}$	2.30	1.84(2)	1.71
$5d_{3/2} \xrightarrow{M2} 5p_{3/2}$	0.0	0.27(1)	
$5d_{3/2} \xrightarrow{E1} 5p_{1/2}$	9.84	7.7(4)	7.24
$5d_{3/2} \xrightarrow{M2} 5p_{1/2}$	5.90	4.9(3)	
$5d_{3/2} \xrightarrow{M1} 6s_{1/2}$	4.8[−12]	2(1)[−9]	
$5d_{3/2} \xrightarrow{E2} 6s_{1/2}$	6.3[3]	4.4(1)[3]	
$6p_{3/2} \xrightarrow{M1} 6p_{1/2}$	1.33	1.33(1)	
$6p_{3/2} \xrightarrow{E2} 6p_{1/2}$	1.64[4]	1.32(1)[4]	
$6p_{3/2} \xrightarrow{E1} 6s_{1/2}$	88.96	72.9(1)	70.3
$6p_{3/2} \xrightarrow{M1} 5p_{3/2}$	4.9[−9]	2.1(5)[−4]	
$6p_{3/2} \xrightarrow{E2} 5p_{3/2}$	131.93	106(8)	
$6p_{3/2} \xrightarrow{M1} 5p_{1/2}$	9.2[−4]	6(1)[−4]	
$6p_{3/2} \xrightarrow{E2} 5p_{1/2}$	96.90	77.3(8)	
$6p_{1/2} \xrightarrow{E1} 6s_{1/2}$	45.81	37.5(1)	36.1
$6p_{1/2} \xrightarrow{M1} 5p_{3/2}$	1.0[−3]	1.4(3)[−3]	
$6p_{1/2} \xrightarrow{E2} 5p_{3/2}$	149.33	120(7)	
$6p_{1/2} \xrightarrow{M1} 5p_{1/2}$	3.9[−10]	1.2(8)[−5]	
$6s_{1/2} \xrightarrow{E1} 5p_{3/2}$	11.26	8.8(2)	8.56
$6s_{1/2} \xrightarrow{E1} 5p_{1/2}$	4.68	3.67(2)	3.64
$5p_{3/2} \xrightarrow{M1} 5p_{1/2}$	1.33	1.31(1)	
$5p_{3/2} \xrightarrow{E2} 5p_{1/2}$	236.42	181(1)	

III. RESULTS AND DISCUSSION

In accordance with Koopman's theorem, the energies of the virtual orbitals obtained in our calculations are the IPs at the DF level, since our DF wave function is computed using the closed-shell configuration $[4p^6]4d^{10}5s^2$. We present the IPs from NIST [10], from other calculations as well as our calculations in Table I.

TABLE III. Wavelengths (λ) in Å, transition rates (A) in s^{-1}, branching ratios (Γ) and lifetimes (τ) in ns for the considered excited states in In. We consider the calculated and experimental values of λs to determine the above quantities which are given as I and II, respectively. We present the recommended (Reco) values for τs after accounting possible errors and compare them with their experimental (Expt.) results. Numbers given in the parentheses and square brackets represent estimated errors and powers in 10, respectively.

Upper	Lower	Channel	$\lambda_{f\to i}$		$A^{O}_{f\to i}$			τ_f			τ_f
state (f)	state (i)	O	I	II	I	II	$\Gamma^{O}_{f\to i}$	I	II	Reco	Expt.
$5d_{5/2}$	$6p_{3/2}$	$E1$	1.09[5]	1.25[5]	48781.17	32544.0	0.0002	6.22	6.27	6.3(2)	7.6(5)[a]
	$6p_{3/2}$	$M2$			6.1[−10]	3.1[−10]	∼0.0				7.1(6)[b]
	$6p_{1/2}$	$M2$	8.23[4]	9.10[4]	4.5[−5]	2.7[−5]	∼0.0				
	$5p_{3/2}$	$E1$	3251	3257	1.61[8]	1.60[8]	0.9998				
	$5p_{3/2}$	$M2$			3.2[−3]	3.2[−3]	∼0.0				
	$5p_{1/2}$	$M2$	3032	3038	8.9[−4]	8.8[−4]	∼0.0				
	$5d_{3/2}$	$M1$	3.38[6]	4.29[6]	2.8[−7]	1.4[−7]	∼0.0				
	$5d_{3/2}$	$E2$			1.2[−12]	3.7[−12]	∼0.0				
	$6s_{1/2}$	$E2$	1.15[4]	1.14[4]	6.10	5.61	∼0.0				
$5d_{3/2}$	$6p_{3/2}$	$E1$	1.13[5]	1.29[5]	7316.78	4935.01	3.0[−5]	5.99	6.03	6.0(3)	6.3(5)[a]
	$6p_{3/2}$	$M2$			7.1[−16]	3.7[−16]	∼0.0				7.0(4)[c]
	$6p_{1/2}$	$E1$	8.43[4]	9.30[4]	8.78[4]	6.55[4]	4.0[−4]				
	$6p_{1/2}$	$M2$		5.7[−11]	3.5[−11]	∼0.0					
	$5p_{3/2}$	$E1$	3254	3259	2.71[7]	2.69[7]	0.16				
	$5p_{3/2}$	$M2$			2.8[−6]	2.7[−6]	∼0.0				
	$5p_{1/2}$	$E1$	3035	3040	1.40[8]	1.39[8]	0.84				
	$5p_{1/2}$	$M2$		7.1[−5]	7.1[−5]	∼0.0					
	$6s_{1/2}$	$M1$	1.16[4]	1.17[4]	1.1[−8]	1.0[−8]	∼0.0				
	$6s_{1/2}$	$E2$			5.99	5.53	∼0.0				
$6p_{3/2}$	$6p_{1/2}$	$M1$	3.34[5]	3.35[5]	2.4[−4]	2.4[−4]	∼0.0	57.67	58.34	58(1)	55(4)[d]
	$6p_{1/2}$	$E2$			8.9[−7]	8.7[−7]	∼0.0				
	$6s_{1/2}$	$E1$	1.29[4]	1.29[4]	1.73[7]	1.71[7]	0.9999				
	$5p_{3/2}$	$M1$	3351	3344	0.04	0.04	∼0.0				
	$5p_{3/2}$	$E2$			69.99	70.73	4.1[−6]				
	$5p_{1/2}$	$M1$	3119	3114	0.13	0.13	∼0.0				
	$5p_{1/2}$	$E2$			73.34	73.93	4.3[−6]				
$6p_{1/2}$	$6s_{1/2}$	$E1$	1.34[4]	1.34[4]	1.58[7]	1.56[7]	0.9999	63.16	63.81	63.8(8)	55(4)[d]
	$5p_{3/2}$	$M1$	3385	3378	0.49	0.49	∼0.0				
	$5p_{3/2}$	$E2$			150.79	152.35	9.7[−6]				
	$5p_{1/2}$	$M1$	3148	3143	0.005	0.005	∼0.0				
$6s_{1/2}$	$5p_{3/2}$	$E1$	4531	4513	9.58[7]	9.70[7]	0.6431	6.71	6.63	6.6(2)	7.5(7)[a]
	$5p_{1/2}$	$E1$	4117	4103	5.33[7]	5.38[7]	0.3569				7.0(3)[e]
											7.4(3)[f]
$5p_{3/2}$	$5p_{1/2}$	$M1$	4.50[4]	4.52[4]	0.0967	0.0957	0.9969	10.31[9]	10.42[9]	10.4(2)[9]	
	$5p_{1/2}$	$E2$			0.0003	0.0003	0.0031				

[a]Reference [11].
[b]Reference [12].
[c]Reference [13].
[d]Reference [14].
[e]Reference [15].
[f]Reference [16].

As observed from Table I, our IP results are within 0.5% except for the $5d$ states (which are around 1% accurate) compared with the results given in [10]. In an earlier work, Safronova *et al.* reported the results for these quantities based on the linearized version of the relativistic CCSD(T) method using a B-spline basis [5]. The major differences between this and our work are the different basis sets used in the two calculations and the additional nonlinear clusters in our calculation. Our results are in better agreement with the high precision NIST results than those of [5] for all the states that we have considered. Given the high accuracy of our IPs and therefore the excitation energies, we can accurately determine the wavelengths for various transitions in order to determine the transition rates and the lifetimes of different excited states. We can also use the wavelengths from NIST data to obtain the lifetimes and compare them with the results from the relativistic CCSD(T) method.

In Table II, we present the line strengths obtained using the DF and relativistic CCSD(T) methods for both the allowed and forbidden transitions. Safronova *et al.* have given the results

only for the allowed transitions [5] and they have not verified explicitly the contributions from the forbidden transitions. In fact, our transition strengths for the allowed transitions differ slightly from theirs and the cause of the differences between the approximations employed in the two cases have already been discussed earlier. The influence of the forbidden transitions should be verified in the determination of transition rates, BRs, and lifetime estimations as they may be important in some cases.

We present the wavelengths, transition rates, branching ratios, and lifetimes of different states of In in Table III. These quantities are determined using both the calculated wavelengths that are estimated from the excitation energies obtained in this work and the experimental wavelengths from NIST data [10]. The *ab initio* results are given as I and wherever the experimental wavelengths are used they are given as II. We also give measured lifetimes results based on different experimental techniques [11–16] in the same table.

The difference between the experimental results and obtained calculations for EEs are treated as possible uncertainties associated with them, which are given in percentage in Table I. Uncertainties in the calculated transition matrix elements are obtained by finding out the contributions from higher angular momentum orbitals using the dominant many-body perturbation diagrams and are mentioned in the parentheses of the results presented in Table II. In the final lifetime estimation of various states, we consider central values given as II in Table III and uncertainties are determined from the above error bars. These results are reported as recommended values (Reco) in Table III.

As we find from the above table, the branching ratios due to the allowed transition channels completely dominate over the forbidden transition channels. Therefore, the lifetimes of the excited states except for the $5p_{3/2}$ state are almost entirely determined by the allowed transitions. The $5p_{3/2}$ state is the fine structure partner of the ground state; its lifetime is determined from the forbidden transitions. For this case, the $M1$ transition clearly dominates over the $E2$ transition and that is evident from their branching ratios. We obtain a large lifetime, $\sim$10 s, for this state. The lifetime of the $5d_{5/2}$ state obtained from our calculation is in reasonable agreement with the available experimental data. We find that the lifetime of this state is almost entirely due to the $E1$ decay channel to $5p_{3/2}$ state. As the wavelength of the transition $5d_{5/2} \rightarrow 6p_{3/2}$ is very large, the branching ratio of this transition is small. Our calculated lifetime for the $5d_{3/2}$ state agrees well with the experimental results. We find 84% and 16% branching ratios from this state to the ground and $5p_{3/2}$ states, respectively, through the $E1$ channel. Contributions from the forbidden transitions are also negligible in this case. Similar agreement between our calculated and experimental results for the lifetimes of the $6p$ states are found, but the experimental results have large error bars compared to our calculations. There is also a marginal difference between the measured lifetimes and the calculated lifetimes of the $6s$ state, although they are within the common error bar. The branching ratios from this state to the ground and $5p_{3/2}$ states are of the order of 35% and 64%, respectively. This trend is different for the $5d_{3/2}$ state as discussed above.

IV. CONCLUSION

We have estimated the branching ratios and lifetimes of certain low-lying excited states of indium. We have carried out calculations of the excitation energies and line strengths using the relativistic coupled-cluster method. We have also compared our *ab initio* results with the results obtained using the experimental wavelengths and measured lifetimes from different experimental techniques. We find that the forbidden transitions do not contribute significantly to the lifetimes of most of the states that we have considered. A large lifetime for the $5p_{3/2}$ state ($\sim$10 s) has been found from this work, which is completely due to the forbidden transitions to its fine structure partner; the ground state.

ACKNOWLEDGMENTS

These calculations were carried out using the Physical Research Laboratory (PRL) high performance computing 3TFLOP cluster at PRL, and the Centre for Development of Advanced Computing (CDAC) Param Padma TeraFlop supercomputer, Bangalore.

[1] B. Klöter, C. Weber, D. Haubrich, D. Meschede, and H. Metcalf, Phys. Rev. A **77**, 033402 (2008).
[2] B. K. Sahoo, R. Pandey, and B. P. Das, Phys. Rev. A (submitted).
[3] T. G. Eck, A. Lurio, and P. Kusch, Phys. Rev. **106**, 954 (1957).
[4] S. George, G. Guppy, and J. Verges, J. Opt. Soc. Am. B **7**, 249 (1990).
[5] U. I. Safronova, M. S. Safronova, and M. G. Kozlov, Phys. Rev. A **76**, 022501 (2007).
[6] N. Vitas, I. Vince, M. A. Lugaro, O. Andriyenko, M. Gosic, and R. J. Rutten, Mon. Not. R. Astron. Soc. **384**, 370 (2008).
[7] C. Jaschek and M. Jaschek, *The Behavior of Chemical Elements in Stars* (Cambridge Publications, Cambridge, 1995).
[8] B. W. Shore and D. H. Menzel, *Principles of Atomic Spectra* (Wiley, New York, 1968).
[9] W. R. Johnson, D. R. Plante, and J. Sapirstein, Adv. At. Mol. Opt. Phys. **35**, 255 (1995).
[10] [http://physics.nist.gov/PhysRefData/Handbook/Tables/indium-table5. tm].
[11] T. Andersen and G. Sorensen, Phys. Rev. A **5**, 2447 (1972).
[12] P. Zimmermann, Z. Phys. **223**, 180 (1969); **226**, 415 (1969).
[13] M. Brieger, H. Bucka, A. Reichelt, and P. Zimmermann, Z. Naturforsch. **24a**, 903 (1969).
[14] M. A. Zaki Ewiss, C. Snoek, and A. Dönszelmann, Astron. Astrophys. **121**, 327 (1983).
[15] M. Norton and A. Gallagher, Phys. Rev. A **3**, 915 (1971).
[16] M. D. Havey, L. C. Balling, and J. J. Wright, J. Opt. Soc. Am. **67**, 491 (1977).